Chapter 4
Soft Power: Stretchable and Ultra-Flexible Energy Sources for Wearable and Implantable Devices

Timothy F. O'Connor, Suchol Savagatrup and Darren J. Lipomi

Abstract The development of ultra-compliant power sources is prerequisite to the realization of imperceptible biomedical systems destined to be worn or implanted in the human body. This chapter assesses the viability of conformal piezo and triboelectric, thermoelectric, and photovoltaic technologies as power sources for biomedical applications. It begins by identifying the amount of energy available to each of these modes of power conversion and then gives a brief overview on the methods of fabricating stretchable electronic devices using deterministic structures, random composites, or molecularly stretchable electronic materials. It then provides a detailed description of innovations in "soft power," where the mentioned design techniques have been employed to develop mechanically compliant power scavengers amenable to integration with stretchable medical devices. The chapter concludes with an analysis of system level power requirements and application specific compatibility, the result of which identifies piezoelectrics and triboelectrics as well suited for intermittent and implantable devices, such as low-power pacemakers for piezoelectrics or higher power wearables and neural stimulators for triboelectrics. Thermoelectrics are highly compatible with epidermal and wearable applications, and can be used as a consistent source of power for tattoo chemical or heat sensors, and photovoltaics can generate large amounts of power in full sun, for high power applications like cochlear implants, or less energy in diffuse or ambient light, for powering hearing aids.

Keywords Stretchable electronics · Stretchable biomedical devices · Wearable power sources · Wearable electronics · Organic electronics · Implantable power sources

T.F. O'Connor · S. Savagatrup · D.J. Lipomi (✉)
Department of NanoEngineering, University of California, 9500 Gilman Drive, Mail Code 0448, La Jolla, San Diego, CA 92093-0448, USA
e-mail: dlipomi@ucsd.edu

J.A. Rogers et al. (eds.), *Stretchable Bioelectronics for Medical Devices and Systems*, Microsystems and Nanosystems,
DOI 10.1007/978-3-319-28694-5_4

4.1 Introduction

An attractive aspect of biointegrated electronics from the standpoint of the research community is the opportunity to reimagine the components of conventional microelectronics [1–7]. Rigid integrated circuits on planar substrates—always connected to a stable source of power—must be transformed into form factors that can conform to the curved and soft surfaces of biological tissue, and which must store or harvest their own power. Delivering, managing, and harvesting energy to power these implantable and wearable devices are critical to the development of this technology [8, 9]. Seamless integration of stretchable power sources into biomedical devices requires the development of "soft power"—highly deformable systems for harvesting and storing energy. This chapter will highlight strategies that enable the design and production of stretchable and ultra-flexible devices for energy harvesting. We define stretchability and ultra-flexibility by the capacity to withstand significant deformation without degradation in performance. We identify four relevant technologies (piezoelectric, triboelectric, thermoelectric, and photovoltaic), their potential applications based on availability of power sources, method of transduction, the performance of the devices (i.e., power output, lifetime of the device, and mechanical properties), and methods of producing them in form factors that are highly deformable.

We preface this chapter by describing the availability of the viable sources of power, Fig. 4.1. Scavenging energy from the human body could potentially be one of the most convenient methods of powering and extending the operation of

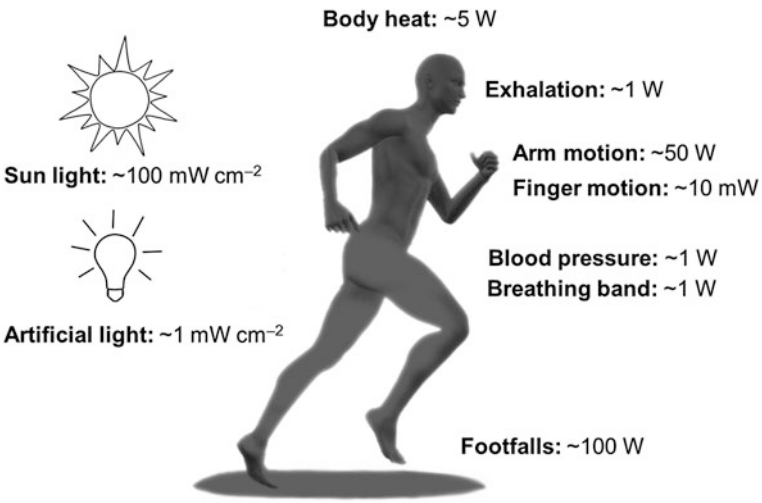

Fig. 4.1 Total power available from body-driven sources in comparison to sunlight and artificial light sources. Adapted from Ref. [10]

biomedical devices [8]. At rest, the human body generates roughly 7 W of power (~5 W from heat, 1 W from breathing, and 1 W from blood pressure) [10]. When in motion, the human body has an additional 100 W of kinetic power available, along with a small amount of power, on the order of 10 mW, that can be collected from small motions of extremities [10]. Physical methods of energy harvesting are usually based on transducers utilizing mechanical energy, such as heart beats [11], blood flow [12], walking [13, 14], breathing [15], and stretching of muscles [16]. Methods of harvesting additional energy from the components of sweat—i.e., bioelectrocatalytic glucose oxidation [17–19]—are exciting developments in the field [20], but our focus is on power that can be harvested from physical motions of the human body and from ambient light. In particular, the sun (which provides around 100 mW cm^{-2} under ideal conditions) and indoor light sources, which can provide power on the order of 1 mW cm^{-2}. Current wearable biomedical devices have power requirements ranging from 1 μW to 10^2 mW, thus the energy available from the human body and external light sources may be sufficient to power these devices [21]. (For the sake of space, we do not cover mechanically compliant devices for energy storage, but direct the reader to the work of others in this area [22–24]).

4.2 Approaches to Making Stretchable Electronics

Three main strategies have been identified for developing stretchable electronics (Fig. 4.2) [25]. The first involves the top-down fabrication of deterministic structures that render otherwise rigid materials (e.g., silicon, metals, and ceramics) stretchable by converting global strains into local deformations of the components on a macroscopic scale. These technologies often use an "island-bridge" approach, whereby rigid components (islands) fabricated on or in a stretchable matrix are connected by fractal or serpentine interconnects (bridges) [26, 27]. Devices can also be compressed to create sinusoidal structures through buckling instabilities [28]. These structures transfer the strain associated with elongation into a decrease in the amplitude (and corresponding increase in the wavelength) of the buckled structures. The second method—random composites—takes advantage of high aspect ratio structures (i.e., nanowires or nanotubes) that form contiguous networks when deposited on or in some elastic support [29–32]. As the device is stretched, one-dimensional structures undergo configurational changes (i.e., rotation, straightening, and sliding past each other), rather than fracturing, allowing electronic performance to be maintained while deformed. Using this method, stretchable electrodes have been fabricated that can accommodate over 400 % strain [33]. The third, complementary approach is intrinsically stretchable electronics, where the active electronic layers themselves accommodate the strain [25, 29, 34]. These

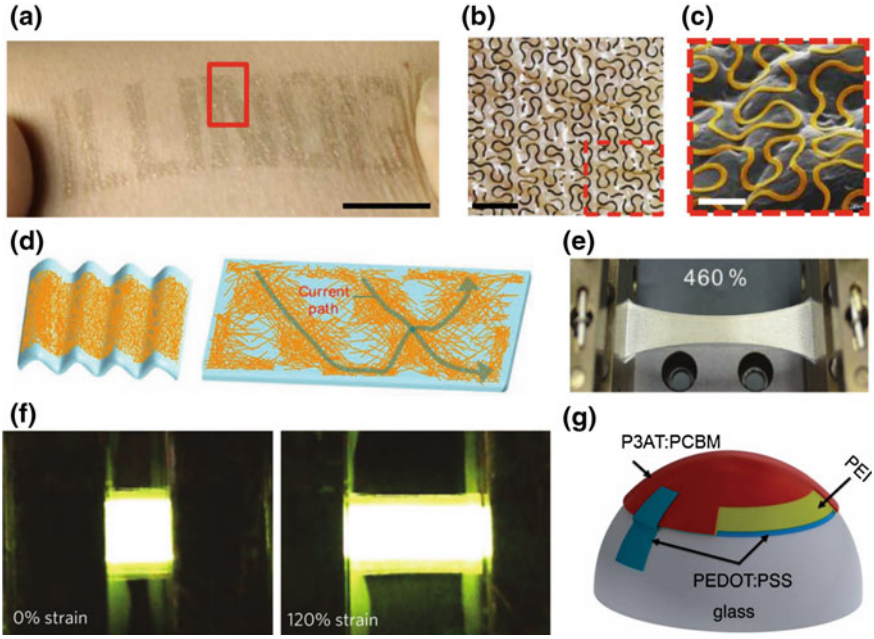

Fig. 4.2 Images of representative samples of strategies for engineering stretchable electronics: deterministic patterning of waves and fractals (**a**–**c**), percolation of random networks and composites (**d**, **e**), and use of intrinsically stretchable elastomer (**f**, **g**). **a** Photograph of metallic wires in a fractal pattern adhered to skin (*scale bar* 1 cm). A *blow-up* within the region indicated by the *red box* is shown in **b** the optical micrograph (*scale bar* 1 mm); and in **c** the scanning electron micrograph (*scale bar* 500 μm). **d** Schematic behavior of the very long Ag NW percolation network (VAgNPN) electrode and an Ecoflex substrate during stretching; **e** photograph of the surface morphology of an electrode on a pre-strained Ecoflex during a 460 % stretching process. **f** Intrinsically stretchable light-emitting devices, employing *Super Yellow*, a poly-phenylenevinylene derivatives. **g** Schematic diagram of hemispherical solar cells using intrinsically stretchable blend of P3AT and PCBM as the active layer. **a**–**c** Reproduced with permission from Ref. [27]. Copyright 2014, Nature Publishing Group **d**, **e** Reproduced with permission from Ref. [33]. Copyright 2012, Wiley-VCH Verlag GmbH & Co. KGaA **f** Reproduced with permission from Ref. [37]. Copyright 2013, Nature Publishing Group **g** Reproduced with permission from Ref. [38]. Copyright 2014, Royal Society of Chemistry

devices are generally made from solution-processable organic materials, which in principle are amenable to high-throughput fabrication techniques [35]. The challenge of intrinsically—or "molecularly" [25]—stretchable systems is that electronic and mechanical properties are generally mutually antagonistic, and thus a material exhibiting state-of-the-art semiconducting properties with the mechanical properties of an elastomer has not yet been demonstrated [36].

4.3 Stretchable Energy Harvesting Technologies

4.3.1 Piezoelectric and Triboelectric

Flexible biomechanical energy harvesters are continuing to show their potential in converting the kinetics of the human body into usable power or signals for devices like pacemakers and pressure sensors, though many of these devices are made of thin films of rigid or brittle ceramics [8, 9, 39–41]. By nature of the transduction mechanism—which only requires physical deformation of the device structure—piezoelectric energy harvesters can be employed as power for both wearable and implantable devices. Due to the intermittency of their energy output and the fact that most of the energy put into the devices is used up to deform the crystal or material structure, piezoelectrics rarely provide the appropriate electronic outputs to continuously operate most biomedical devices without storage [8]. However, piezoelectrics can be used to extend the lifetime of implantable devices, and highly sensitive piezoelectrics can directly transduce physical stimuli for sensors that require no external power supplies [8]. Most high-performance piezoelectric materials are brittle with high-tensile moduli [42]; and the devices reviewed here are the state of the art for stretchable or soft piezoelectrics.

In work by McAlpine and co-workers, brittle lead zirconate titanate (PZT, Pb $[Zr_{0.52}TI_{0.48}]O_3$) nanoribbons were deterministically patterned into wave-like structures, allowing for flexing and stretching operating modes by transferring the mechanical strain to the amplitudes and wavelength of the buckled structures (Fig. 4.3a–c) [42]. The buckled PZT nanoribbons exhibited nearly a two order of magnitude increase in maximum tensile strain without failure over the non-buckled counterparts, 8 % versus 0.1 %, by transferring the elongation to a reduction in the amplitude of the waves. Moreover, the structures also exhibited an enhanced electromechanical performance attributed to a flexoelectric contribution to the piezoelectric coefficient, leading to the peak power density of 2.5 W cm^{-3} under uniaxial deformation [42].

Examples of high performance devices exhibiting biaxial stretchability typically comprise functional nanocomposites in elastomeric substrates. Yao and coworkers demonstrated lead magnesium niobate-lead titanate (PMN-PT) nanoclusters (Fig. 4.3d–f) embedded in elastomeric substrates that generated voltages ranging from 4.2 to 7.8 V in an open circuit and currents ranging from 1.58 to 2.29 μA, yielding maximum instantaneous power outputs of roughly 36 μW cm^{-2} [43]. The lowest strain in these devices that produced a piezoelectric response was ~0.01 %, making them promising for applications in self-powered pressure sensors. Similarly, Huang et al. developed wearable triboelectric nanogenerators capable of harnessing highly available energy from walking (Fig. 4.3g–i) [44]. The all-fiber PVDF insoles were fabricated by electrospinning, which produced fibrils with nanostructured features that improved triboelectric performance. At a step

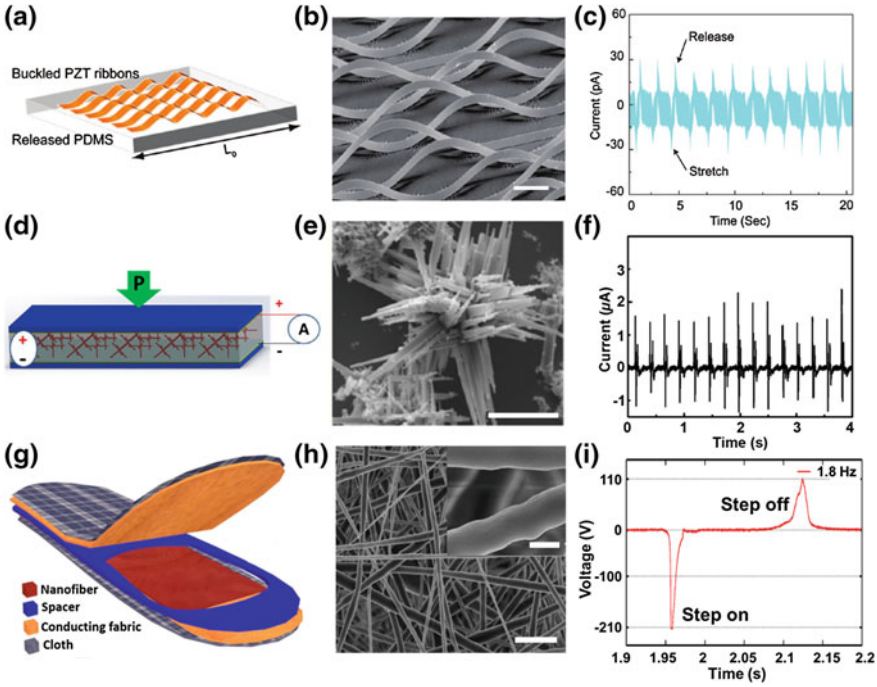

Fig. 4.3 Representative examples of piezoelectric and triboelectric devices that are possible for biointegration. **a** Schematic of lead zirconate titanate (PZT) nanoribbons and **b** scanning electron micrograph of the PZT ribbons transfer-printed to prestrained elastomeric substrate that produced the buckling morphology (*scale bar* 20 μm). **c** Short-circuit current measured from devices comprising 5 PZT ribbons under periodic stretching of 8 % strain. **d** Schematic of PMN-PT nanowire-based nanocomposite comprising PMN-PT nanowires embedded in elastomeric substrate, PDMS, and polyimide/gold electrodes. **e** High-magnification scanning electron micrograph of dispersed PMN-PT nanowires (*scale bar* 5 μm). **f** Signal generation from PMN-PT nanocomposite showing the current generation under a periodic mechanical tapping. **g** Schematic diagram of the wearable all-fiber triboelectric nanogenerator (TENG)-based insole composed of electrospun piezoelectric polyvinylidene fluoride (PVDF) nanofibers. **h** Scanning electron micrograph PVDF nanofibers (*scale bar* 10 μm; *inset scale bar* 500 nm). **i** Voltage-time curve corresponding to the mechanical stimuli. **a**–**c** Reproduced with permission from Ref. [42]. Copyright 2011, American Chemical Society. **d**–**f** Reproduced with permission from Ref. [43]. Copyright 2013, American Chemical Society. **g**–**i** Reproduced with permission from Ref. [44]. Copyright 2015, Elsevier Ltd

frequency of 1.8 Hz (or typical walking speed of $\sim$4 km h^{-1} with an average stride length), the devices produced a maximum output voltage, instantaneous power, and output current of 210 V, 2.1 mW, and 45 μA, respectively [44]. The active materials take the form of nanowoven fabrics that can be integrated into mechanoelectric textiles, including shirts, pants, and insoles [44, 45]. These devices can be potentially used to charge batteries or for neural stimulators [8].

4.3.2 Thermoelectric

Thermoelectric power generators (TEGs) can provide continuous power to wearable or subdermal biomedical devices and sensors. Unlike piezoelectric and triboelectric devices, TEGs offer a means of continuous, stable power, however they are limited by the small temperature gradients afforded by the limitations of human tolerance (between 2 and 5 K) and loss of latent heat through evaporation of sweat [13]. Notwithstanding these limitations, a lightweight, flexible TEG module was recently reported by Cho and coworkers [46, 47]. The device comprised a screen-printed inorganic porous thick film of n-type bismuth telluride (Bi_2Te_3) and p-type antimony telluride (Sb_2Te_3), infiltrated with poly(3,4-ethylenedioxythiophene):poly(styrenesulfonate) (PEDOT:PSS) to increase the electrical conductivity and provide mechanical flexibility. With the addition of PEDOT:PSS in the composite TEGs exhibited a 10 % increase in the dimensionless figure of merit (ZT) over their screen printed, purely inorganic counterparts, and maintained high conductivity when devices were bent to 3 cm radii of curvature (Fig. 4.4a–b). At a temperature difference of 10 K, with the cold side held at 283 K, devices generated an output voltage of 19.1 mV and an output power density of 60 μW cm^{-2} [46]. To demonstrate the

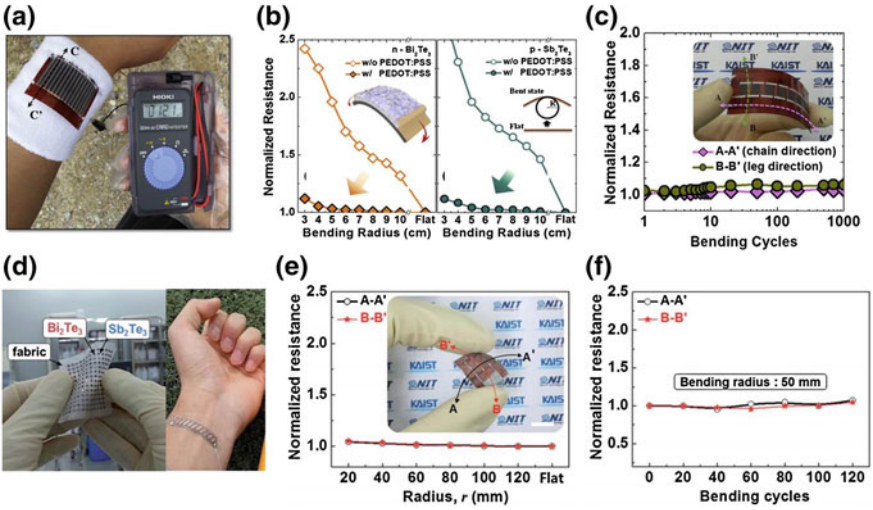

Fig. 4.4 Wearable thermoelectric devices. **a–c** Hybrid inorganic-organic composite thermoelectric modules. **a** Device in operation on the human body. **b** Normalized resistance changes before (open points) and after (closed points) PEDOT:PSS infiltration as a function of bending radius for Bi_2Te_3 (*left*) and Sb_2Te_3 (*right*). **c** Resistance changes of the module as a function of the number of bending cycles with a bending radius of 40 mm. **d–f** Wearable thermoelectric generator fabricated on a glass fabric. **d** Image of 196 Bi_2Te_3 and Sb_2Te_3 dots on glass fabric of 40 mm × 40 mm (*left*) and a complete device mounted on human skin (*right*). **e** Resistance stability of the device under bending stress along two bending axes as a function of bending radius. **f** Stability of 120 bending cycles at bending radius of 50 mm. **a–c** Reproduced with permission from Ref. [46]. Copyright 2014, Elsevier Ltd. **d–f** Reproduced with permission from Ref. [47]. Copyright 2014, Royal Society of Chemistry

mechanical endurance and potential for wearable energy applications, a TEG consisting of seven thermoelectric couples was subjected to cyclic mechanical bending (radius of curvature of 4 cm) of over 1,000 cycles. Figure 4.4c shows fatigue strength of the device, which only exhibits minimal increase in resistance.

In another study by the same group, Kim et al. improved the mechanical compliance of the TEGs by screen printing dots of Bi_2Te_3 and Sb_2Te_3 onto a woven glass fabric and subsequently sealed inside a PDMS encapsulant (Fig. 4.4d) [47]. The glass fabric, which served as a mechanically compliant substrate, also increased power generation by interrupting phonon propagation, thus reducing the thermal conductivity of the printed TE films. To demonstrate the use of this technology as a power source for wearable biomedical devices, a device comprising 11 thermocouples in the shape of a bandage was bonded to the surface of the skin. The device created an output power of 3 μW, with an open circuit voltage of 2.9 mV, on a matched external load with an air temperature of 15 °C [47]. A similar prototype consisting of eight couples was subjected to mechanical testing, whereby the device showed no significant change (<5 %) in the internal resistance with the allowed bending radius of 20 mm; furthermore, devices showed <7 % decrease in internal resistance when repeatedly bent up to 120 cycles with a radius of curvature of 50 mm (Fig. 4.4e–f) [47]. The reported power density is sufficient to activate sub-microwatt or microwatt wearable devices such as a temperature sensor or a CMOS image sensor [47].

4.3.3 Photovoltaic Devices

Unlike the two previous sections in which the energy outputs are limited by scavenging physical and thermal energy sources of the human body, photovoltaic (PV) devices have the potential to produce substantially more energy than piezoelectric and thermoelectric devices. However, the main limitations of PV devices for wearable applications will most likely be (1) the availability and the intensity of the light sources and (2) the surface area required for the photoactive components. The power output of PV devices will be significantly lower under diffuse outdoor light or ambient indoor light rather than ideal sunlight, and for devices with modest efficiency, larger active areas will be required for a viable power output. Despite the challenges related to indoor power, several photovoltaic technologies can be made in ultra-flexible or stretchable form factors while still providing useful power densities [48].

Crystalline semiconductors of which most high performing solar cells are composed are extremely brittle; however, careful engineering of the materials and creative approaches to the layout of the devices can significantly increase the deformability of whole modules. One of the first examples of stretchable solar cells was introduced by Rogers and coworkers by exploiting the "island-bridge" approach [49]. Gallium arsenide (GaAs) solar cells (roughly $\sim$3.6 μm thick) were transfer-printed onto prestrained elastomeric PDMS substrate with thin gold interconnects between active devices (Fig. 4.5a–b) [49]. Trenches between each active device absorbed the strains

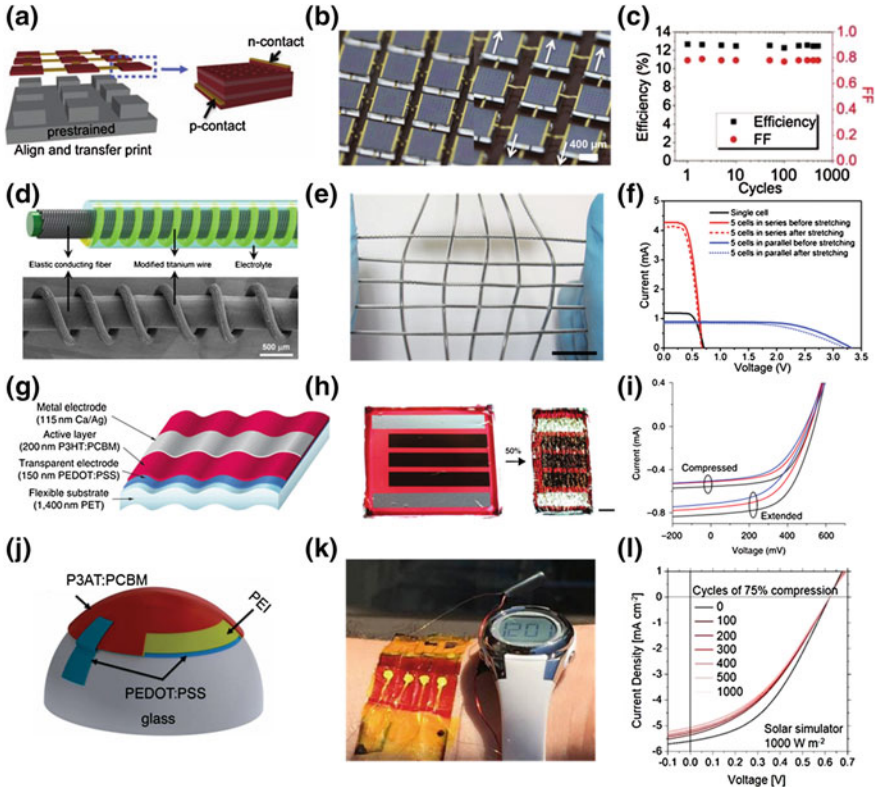

Fig. 4.5 Stretchable photovoltaic devices. **a–c** Stretchable GaAs solar cells fabricated on "island-bridge" architecture **a** Schematic diagram. **b** Unstretched cells (*left*) and 20 % biaxial strain (*right*). **c** Device performance as a function of the number of stretching cycle at 20 % biaxial strain. **d–f** Stretchable and wearable dye-sensitized solar cells comprising elastic conducting fiber, modified titanium wire, and electrolyte. **d** Schematic diagram and scanning electron micrograph of the device. **e** Photograph of a stretchable photovoltaic textile after stretching (*scale bar* 2 cm). **f** *J–V curves* of the photovoltaic textile in series and parallel before and after stretching. **g–i** Organic solar cells fabricated on ultra-thin polyester substrates. **g** Schematic diagram. **h** Prestrained substrate of ultra-thin polyester at flat (*left*) and 50 % (*right*) quasi-linear compression (*scale bar* 2 mm). **i** Device performance for 1 (*black*), 11 (*red*), and 22 (*blue*) cycles for both the fully extended and 50 % compressed states. **j** Hemispherical solar cells using intrinsically stretchable blend of P3AT and PCBM as the active layer. **k** Wearable, ultra-flexible organic solar cells comprising the composite of P3HpT:PCBM powering a digital watch in natural sunlight (98 mW cm^{-2}). (l) The performance of wearable organic solar cells measured in air over 1,000 cycles of 75 % compressive strain. **a–c** Reproduced with permission from Ref. [49]. Copyright 2011, Wiley-VCH Verlag GmbH & Co. KGaA. **d–f** Reproduced with permission from Ref. [50]. Copyright 2014, Wiley-VCH Verlag GmbH & Co. KGaA. **g–i** Reproduced with permission from Ref. [51]. Copyright 2012 Nature Publishing Group. **j** Reproduced with permission from Ref. [38]. Copyright 2014, Royal Society of Chemistry. **k–l** Reproduced with permission from Ref. [52]

caused by bending or stretching of the devices, allowing biaxial stretching of 20 % strain (over 500 cycles) without degradation in performance (Fig. 4.5c) [49]. These devices performed identically in the relaxed and stretched states, providing the power conversion efficiency (*PCE*) under one sun condition (100 mW cm^{-2}) of ~13 % (13 mW cm^{-2}) [49]. Another example of transforming rigid materials into stretchable devices was described by Peng and coworkers; dye-sensitized solar cells were fabricated in a spring-like architecture to accommodate 30 % uniaxial strain (Fig. 4.5d–e) [50]. The solar cell consisted of two stretchable fiber electrodes (a rubber fiber wrapped with conductive multi-walled carbon nanotube sheets and a modified active titanium wire), both of which were encapsulated by a transparent polyethylene tube. The device was completed by filling the cavity of the tube with a liquid redox electrolyte and sealing the device [50]. A single cell of the wire-like solar harvester exhibited *PCE* of 7.13 % when unstretched [50]. Multiple devices were assembled into a stretchable "photovoltaic textile" comprising five cells connected in series and parallel. This assembly performed similarly when stretched and retained ~90 % of its original efficiency when subjected to 50 cycles of 20 % strain (Fig. 4.5f) [50].

Unlike the previous two examples, organic photovoltaics are typically much thinner (roughly ~200 nm); this thinness drastically increases the flexibility (provided a sufficiently thin substrate is used). In one of the most impressive demonstrations of ultra-flexibility of organic solar cells to date, Kaltenbrunner et al. fabricated ultra-thin organic solar cells based on a composite of poly (3-hexylthiophene) and [6,6]-phenyl C_{61} butyric acid methyl ester (P3HT:PCBM) on a 1.4 μm polyester foil (Fig. 4.5a) [51]. This solar cell holds the current record for specific power of organic solar cells (10 W g^{-1}) and can achieve bending radii of ~35 μm [51]. Using a similar approach to that described earlier by Lipomi et al. [53] the authors showed that the devices can also be reversibly compressed to 50 % of their original size when bonded to prestretched elastomeric substrates (Fig. 4.5b). Under one sun illumination (100 mW cm^{-2}), the *PCE* was measured to be around 4 % (or power density of 4 mW cm^{-2}) before deformation, and around 3 % (3 mW cm^{-2}) after 22 cycles of 50 % compression (Fig. 4.5c) [51].

Recently, our laboratory reported stretchable solar cells capable of being conformally bonded to hemispherical surfaces (Fig. 4.5j) [38]. The all-organic, fully stretchable solar cell, comprising a composite of poly(3-octylthiophene) and PCBM (P3OT:PCBM), was prefabricated onto an elastomeric substrate, then transferred to a glass hemispherical surface through contact printing. The study was a demonstration of the significant increase in compliance of the resulting devices by increasing the molecular side chain length of semiconducting polymers [54]. Devices, fabricated from a composite of P3HT:PCBM (P3HT has six carbon atoms per side chain, $n = 6$), have superior electrical performance on a flat configuration but cracked under modest strain; while devices comprising P3OT:PCBM ($n = 8$) performed worse on flat substrates but retained functionality when applied onto hemispherical substrate (conformal bonding required the solar cell to be stretched by ~24 % strain) [38]. Additionally, we found that poly(3-heptylthiophene) and PCBM (P3HpT:PCBM, $n = 7$) exhibited both high charge carrier mobilities and

high compliance [36], enabling us to fabricate an ultra-flexible, wearable organic solar cells capable of powering wearable devices [52]. This ultra-flexible device conforms to the human body and generated uninterrupted power over repeated compressive strain of 75 % and a tensile strain of 5 % [52]. These wearable solar cells provided up to 500 μW (power density of 1 mW cm^{-2}) when measured with natural sunlight (98 mW cm^{-2}), and ~5 μW (power density of 10 μW cm^{-2}) when measured indoors in diffuse artificial light [52]. These devices are promising for applications such as powering wearable applications (e.g., wearable biosensors) due to their relatively high power density, high specific power, and extreme mechanical durability.

4.4 System Level Power Requirements

While we introduced many examples of power generation devices, it is crucial to address the viability of each option by evaluating its compatibility with different biomedical applications. We will base our discussion on the power generation capability of the power sources and the feasibility of incorporating them onto the given applications. Figure 4.6 highlights the examples of several biomedical devices and the range of their typical power consumption, along with the range of energy generation for the technologies outlined previously in the chapter. Photovoltaic devices, under a full sun, could produce substantial amount of power to meet the typical power consumption of most biomedical devices [21]. For example, given an active area of 100 cm^2 (roughly the size of standard index card),

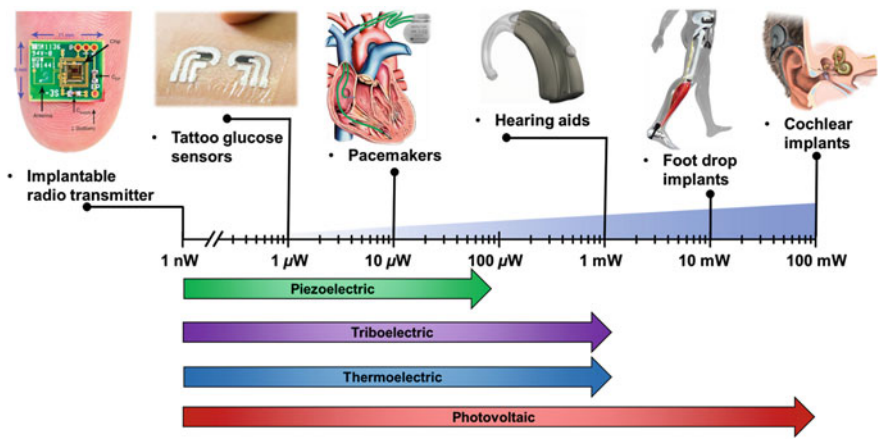

Fig. 4.6 Order of magnitude of typical power consumption of biomedical devices and the range of power generation by the four technologies outlined in this chapter. Images reproduced with permission from Ref. [58], copyright 2012, Nature Publishing Group. Images adapted from Refs. [21, 56, 57, 60]

organic solar cells can potentially produce 300 mW while GaAs solar cells upward of 1.3 W. Purely from the energy production standpoint, these PV devices would be able to power hearing aids, foot-drop implants [55, 56], and cochlear implants [57]. However, this energy production would be approximately two orders of magnitude lower in diffuse light and nonexistent without a light source. In addition, integration of PV devices and implantable devices will not be seamless and overcoming the users' barriers in terms of appeal, aesthetics, and comfort poses further challenges. Thermoelectric devices would be ideal to provide continuous power generation; despite the low efficiency arising from the low temperature gradient the body can endure, the power generated can be used to power small electronics and biosensors. For example, Mercier et al. fabricated an extremely low-power implantable chip that measures the endocochlear potential and transmits the measurement via a 2.4 GHz radio signal while consuming power on the order of 1 nW [58]. Tattoo-based technology, whose operating locations coincide with the largest temperature gradient on the human body, may also benefit from thermoelectric power generators. Epidermal electronics incorporate many electronic functionalities (e.g., temperature and strain sensors, transistors, light-emitting diodes, photodetectors, and radio frequency inductors) [59] and medical applications (e.g., pH sensor, sodium sensor, and ammonium sensor) [19, 60]. Piezoelectric and triboelectric devices provide possible sources of power for implantable devices that only consume energy intermittently. The main example is powering pacemakers by harvesting energy from the motions of the heart [61]. Improvements on current pacemakers are also aimed at reducing the power consumption by almost an order of magnitude [12, 62]. Also, the large amount of kinetic energy available in foot-falls makes triboelectric generators a viable technology for foot-drop neural stimulators, where energy generation and signal transduction could be performed simultaneously.

4.5 Conclusions and Challenges

Ultra-flexible and stretchable power sources will be essential components of future biointegrated medical devices. We have described several methods of energy harvesting that are compatible with biointegration; making devices compatible with soft, biological structures is tantamount to rendering them extraordinarily mechanically compliant. Before seamless integration between biomedical devices and power generators can be realized, more collaborative and multidisciplinary studies between the two fields of biology and electronics will be required. Understanding the transitional steps to bridge the two sides of science and engineering will most likely produce fruitful discovery and unexpected problems that could potentially bring us closer to fully functional and self-powered biomedical devices.

References

1. D.-H. Kim, J.A. Rogers, Adv. Mater. **20**, 4887 (2008)
2. J.A. Rogers, T. Someya, Y. Huang, Science **327**, 1603 (2010)
3. D.-H. Kim, J. Song, W.M. Choi, H.-S. Kim, R.-H. Kim, Z. Liu, Y.Y. Huang, K.-C. Hwang, Y. Zhang, J. Rogers, Proc. Natl. Acad. Sci. U.S.A. **105**, 18675 (2008)
4. M. Kaltenbrunner, T. Sekitani, J. Reeder, T. Yokota, K. Kuribara, T. Tokuhara, M. Drack, R. Schwödiauer, I. Graz, S. Bauer-Gogonea, S. Bauer, T. Someya, Nature **499**, 458 (2013)
5. D. Ghezzi, M.R. Antognazza, R. Maccarone, S. Bellani, E. Lanzarini, N. Martino, M. Mete, G. Perile, S. Bisti, G. Lanzani, F. Benfenati, Nat. Photon. **7**, 400 (2013)
6. L. Xu, S.R. Gutbrod, A.P. Bonifas, Y. Su, M.S. Sulkin, N. Lu, H.-J. Chung, K.-I. Jang, Z. Liu, M. Ying, C. Lu, R.C. Webb, J.-S. Kim, J.I. Laughner, H. Cheng, Y. Liu, A. Ameen, J.-W. Jeong, G.-T. Kim, Y. Huang, I.R. Efimov, J. Rogers, Nat. Commun. **5**, 3329 (2014)
7. T.F. O'Connor, K.M. Rajan, A.D. Printz, D.J. Lipomi, Mater. Chem. B **3**, 4947 (2015)
8. C.Y. Sue, N.C. Tsai, Appl. Energy **93**, 390 (2012)
9. J. Yun, S.N. Patel, M.S. Reynolds, G.D. Abowd, IEEE Trans. Mob. Comput. **10**, 669 (2011)
10. T. Starner, IBM Syst. J. **35**, 618 (1996)
11. Z. Li, G. Zhu, R. Yang, A.C. Wang, Z.L. Wang, Adv. Mater. **22**, 2534 (2010)
12. M. Deterre, E. Lefeuvre, Y. Zhu, M. Woytasik, B. Boutaud, R.D.J. Molin, Microelectromech. Syst. **23**, 651 (2014)
13. R. Riemer, A. Shapiro, J. Neuroeng. Rehabil. **8**, 22 (2011)
14. L.C. Rome, L. Flynn, E.M. Goldman, T.D. Yoo, Science **309**, 1725 (2005)
15. C. Sun, J. Shi, D.J. Bayerl, X. Wang, Energy Environ. Sci. **4**, 4508 (2011)
16. R. Yang, Y. Qin, C. Li, G. Zhu, Z.L. Wang, Nano Lett. **9**, 1201 (2009)
17. V. Coman, R. Ludwig, W. Harreither, D. Haltrich, L. Gorton, T. Ruzgas, S. Shleev, Fuel Cells **10**, 9 (2010)
18. C. Pan, Y. Fang, H. Wu, M. Ahmad, Z. Luo, Q. Li, J. Xie, X. Yan, L. Wu, Z.L. Wang, J. Zhu, Adv. Mater. **22**, 5388 (2010)
19. A.J. Bandodkar, W. Jia, J. Wang, Electroanalysis **27**, 562 (2015)
20. E. Katz, in, ed. by E. Katz, *Implantable Bioelectronics* (Wiley-VCH Verlag GmbH & Co. KGaA, 2014), p. 363
21. M. Deterre, *Toward an Energy Harvester for Leadless Pacemakers* (University of Paris-Sud, 2013)
22. M. Kaltenbrunner, G. Kettlgruber, C. Siket, R. Schwödiauer, S. Bauer, Adv. Mater. **22**, 2065 (2010)
23. S. Xu, Y. Zhang, J. Cho, J. Lee, X. Huang, L. Jia, J.a Fan, Y. Su, J. Su, H. Zhang, H. Cheng, B. Lu, C. Yu, C. Chuang, T.-I. Kim, T. Song, K. Shigeta, S. Kang, C. Dagdeviren, I. Petrov, P. V. Braun, Y. Huang, U. Paik, J.A. Rogers, Nat. Commun. **4**, 1543 (2013)
24. L. Hu, H. Wu, F. La Mantia, Y. Yang, Y. Cui, ACS Nano **4**, 5843 (2010)
25. S. Savagatrup, A.D. Printz, T.F. O'Connor, A.V. Zaretski, D.J. Lipomi, Chem. Mater. **26**, 3028 (2014)
26. S.P. Lacour, J. Jones, S. Wagner, Proc. IEEE **93**, 1459 (2005)
27. J. Fan, W.-H. Yeo, Y. Su, Y. Hattori, W. Lee, S.-Y. Jung, Y. Zhang, Z. Liu, H. Cheng, L. Falgout, M. Bajema, T. Coleman, D. Gregoire, R.J. Larsen, Y. Huang, J. Rogers, Nat. Commun. 5, 3266 (2014)
28. D.-Y. Khang, J.a. Rogers, H.H. Lee, Adv. Funct. Mater. **19**, 1526 (2009)
29. Z. Yu, X. Niu, Z. Liu, Q. Pei, Adv. Mater. **23**, 3989 (2011)
30. J. Liang, L. Li, K. Tong, Z. Ren, W. Hu, X. Niu, Y. Chen, Q. Pei, ACS Nano **8**, 1590 (2014)
31. D.J. Lipomi, M. Vosgueritchian, B.C.-K. Tee, S.L. Hellstrom, J.A. Lee, C.H. Fox, Z. Bao, Nat. Nanotech. **6**, 788 (2011)
32. S.P. Lacour, D. Chan, S. Wagner, T. Li, Z. Suo, Appl. Phys. Lett. **88**, 204103 (2006)
33. P. Lee, J. Lee, H. Lee, J. Yeo, S. Hong, K.H. Nam, D. Lee, S.S. Lee, S.H. Ko, Adv. Mater. **24**, 3326 (2012)

34. G. Kettlgruber, M. Kaltenbrunner, C.M. Siket, R. Moser, I.M. Graz, R. Schwödiauer, S. J. Bauer, Mater. Chem. A **1**, 5505 (2013)
35. F.C. Krebs, N. Espinosa, M. Hösel, R.R. Søndergaard, M. Jørgensen, Adv. Mater. **26**, 29 (2014)
36. S. Savagatrup, A.D. Printz, H. Wu, K.M. Rajan, E.J. Sawyer, A.V. Zaretski, C.J. Bettinger, D. J. Lipomi, Synth. Met. **203**, 208 (2015)
37. J. Liang, L. Li, X. Niu, Z. Yu, Q. Pei, Nat. Photonics **7**, 817 (2013)
38. T.F. O'Connor, A.V. Zaretski, B.A. Shiravi, S. Savagatrup, A.D. Printz, M.I. Diaz, D. J. Lipomi, Energy Environ. Sci. **7**, 370 (2014)
39. G.T. Hwang, H. Park, J.H. Lee, S. Oh, KIl Park, M. Byun, H. Park, G. Ahn, C.K. Jeong, K. No, H. Kwon, S.G. Lee, B. Joung, K. Lee, J. Adv. Mater. **26**, 4880 (2014)
40. Y. Qi, M.C. McAlpine, Energy Environ. Sci. **3**, 1275 (2010)
41. M. Lee, C.Y. Chen, S. Wang, S.N. Cha, Y.J. Park, J.M. Kim, L.J. Chou, Z.L. Wang, Adv. Mater. **24**, 1759 (2012)
42. Y. Qi, J. Kim, T.D. Nguyen, B. Lisko, P.K. Purohit, M.C. McAlpine, Nano Lett. **11**, 1331 (2011)
43. S. Xu, Y.W. Yeh, G. Poirier, M.C. McAlpine, R.A. Register, N. Yao, Nano Lett. **13**, 2393 (2013)
44. T. Huang, C. Wang, H. Yu, H. Wang, Q. Zhang, M. Zhu, Nano Energy **14**, 226 (2015)
45. C.K. Jeong, J. Lee, S. Han, J. Ryu, G.-T. Hwang, D.Y. Park, J.H. Park, S.S. Lee, M. Byun, S. H. Ko, K. Lee, J. Adv. Mater. **27**, 2866 (2015)
46. J.H. We, S.J. Kim, B.J. Cho, Energy **73**, 506 (2014)
47. S.J. Kim, J.H. We, B.J. Cho, Energy Environ. Sci. **2014**, 7 (1959)
48. D.J. Lipomi, Z. Bao, Energy Environ. Sci. **4**, 3314 (2011)
49. J. Lee, J. Wu, M. Shi, J. Yoon, SIl Park, M. Li, Z. Liu, Y. Huang, J.A. Rogers, Adv. Mater. **23**, 986 (2011)
50. Z. Yang, J. Deng, X. Sun, H. Li, H. Peng, Adv. Mater. **26**, 2643 (2014)
51. M. Kaltenbrunner, M.S. White, E.D. Głowacki, T. Sekitani, T. Someya, N.S. Sariciftci, S. Bauer, Nat. Commun. **3**, 770 (2012)
52. T.F. O'Connor, A.V. Zaretski, S. Savagatrup, A.D. Printz, C.D. Wilkes, M.I. Diaz, E. J. Sawyer, D.J. Lipomi, Sol. Energy Mater. Sol. Cells **144**, 438 (2016)
53. D.J. Lipomi, B.C.-K. Tee, M. Vosgueritchian, Z. Bao, Adv. Mater. **23**, 1771 (2011)
54. S. Savagatrup, A.S. Makaram, D.J. Burke, D.J. Lipomi, Adv. Funct. Mater. **24**, 1169 (2014)
55. M. Haugland, C. Childs, M. Ladouceur, J. Haase, T. Sinkjaer, in *Proceedings of the 5th Annual IFESS Conference* (2000), p. 59
56. G.M. Lyons, T. Sinkjær, J.H. Burridge, D.J. Wilcox, IEEE Trans. Neural Syst. Rehabil. Eng. **10**, 260 (2002)
57. M.W. Baker, *A Low-Power Cochlear Implant System, Massachusetts Institute of Technology* (2007)
58. P.P. Mercier, A.C. Lysaght, S. Bandyopadhyay, A.P. Chandrakasan, K.M. Stankovic, Nat. Biotechnol. **30**, 1240 (2012)
59. D.-H. Kim, N. Lu, R. Ma, Y.-S. Kim, R.-H. Kim, S. Wang, J. Wu, S.M. Won, H. Tao, A. Islam, K.J. Yu, T. Kim, R. Chowdhurry, M. Ying, L. Xu, M. Li, H.-J. Chung, H. Keum, M. McCormick, P. Liu, Y.-W. Zhang, F.G. Omenetto, Y. Huang, T. Coleman, J.A. Rogers, Science **333**, 838 (2011)
60. A.J. Bandodkar, W. Jia, C. Yard, X. Wang, J. Ramirez, J. Wang, Anal. Chem. **87**, 394 (2015)
61. C. Dagdeviren, B.D. Yang, Y. Su, P.L. Tran, P. Joe, E. Anderson, J. Xia, V. Doraiswamy, B. Dehdashti, X. Feng, B. Lu, R. Poston, Z. Khalpey, R. Ghaffari, Y. Huang, M.J. Slepian, J. Rogers, Proc. Natl. Acad. Sci. U. S. A. **2014**, 111 (1927)
62. M. Deterre, B. Boutaud, R. Dalmolin, S. Boisseau, J.-J. Chaillout, E. Lefeuvre, E. Dufour-Gergam, in *2011 Symposium on Design, Test, Integration and Packaging of MEMS/MOEMS (DTIP)* (2011), p. 387